

Linear Versus Geometric Morphometric Approaches for the Analysis of Head Shape Dimorphism in Lizards

Anne-Claire Fabre,¹ Raphaël Cornette,² Katleen Huyghe,³ Denis V. Andrade,⁴ and Anthony Herrel^{5,6*}

¹Department of Evolutionary Anthropology, Duke University, Durham, North Carolina 27708-0383

²Origine, Structure et Evolution de la Biodiversité, UMR 7205, CNRS/MNHN, 45 rue Buffon, Paris 75005, France

³Department of Biology, University of Antwerp, Antwerpen B-2610, Belgium

⁴Departamento de Zoologia, Universidade Estadual Paulista, Rio Claro, c. p. 199, São Paulo 13506-900, Brazil

⁵Département d'Ecologie et de Gestion de la Biodiversité, 55 rue Buffon, CP 55, 75005 Paris Cedex 5, France

⁶Evolutionary Morphology of Vertebrates, Ghent University, Ghent B-9000, Belgium

ABSTRACT Differences between the sexes may arise because of differences in reproductive strategy, with females investing more in traits related to reproductive output and males investing more in traits related to resource holding capacity and territory defence. Sexual dimorphism is widespread in lizards and in many species males and females also differ in head shape. Males typically have bigger heads than females resulting in intersexual differences in bite force. Whereas most studies documenting differences in head dimensions between sexes use linear dimensions, the use of geometric morphometrics has been advocated as more appropriate to characterize such differences. This method may allow the characterization of local shape differences that may have functional consequences, and provides unbiased indicators of shape. Here, we explore whether the two approaches provide similar results in an analyses of head shape in *Tupinambis merianae*. The Argentine black and white tegu differs dramatically in body size, head size, and bite force between the sexes. However, whether the intersexual differences in bite force are simply the result of differences in head size or whether more subtle modifications (e.g., in muscle insertion areas) are involved remains currently unknown. Based on the crania and mandibles of 19 lizards with known bite force, we show intersexual differences in the shape of the cranium and mandible using both linear and geometric morphometric approaches. Although both types of analyses showed generally similar results for the mandible, this was not the case for the cranium. Geometric morphometric approaches provided better insights into the underlying functional relationships between the cranium and the jaw musculature, as illustrated by shape differences in muscle insertion areas not detected using linear morphometric data. *J. Morphol.* 275:1016–1026, 2014. © 2014 Wiley Periodicals, Inc.

KEY WORDS: bite force; sexual dimorphism; head shape

INTRODUCTION

Differences between the sexes may arise because of differences in reproductive strategy with females investing more in traits directly related to fecundity, and males investing more in traits

related to territory defense and/or resource holding capacity (Andersson, 1994). Sexual dimorphism is widespread in lizards with males typically being larger than females, but females often having a larger abdomen (Braña, 1996). Moreover, in many lizards, males and females differ in head shape with males often having bigger heads than females (see Vincent and Herrel, 2007; but see Herrel et al., 2014). Given that larger heads can accommodate more jaw muscles, the observed dimorphism in head size often is related to an intersexual difference in bite force (Herrel et al., 1999; Lappin et al., 2006; Brecko et al., 2008; Vanhooydonck et al., 2007). Although the selective pressures underlying the observed dimorphism in bite force are often difficult to identify, both male–male combat (e.g., Huyghe et al., 2005; Lappin and Husak, 2005) and dietary niche divergence (see review in Vincent and Herrel, 2007) have been suggested as possible drivers of sexual head shape and bite force dimorphisms.

Whereas most studies documenting differences in head dimensions between the sexes use linear dimensions to characterize head size and shape (Herrel et al., 1999; Metzger and Herrel, 2005;

Contract grant sponsors: Conselho Nacional de Desenvolvimento Científico e Tecnológico (CNPq), Fundação de Amparo a Pesquisa do Estado de São Paulo (FAPESP), and Fundação para o Desenvolvimento da Universidade Estadual Paulista (FUNDUNESP; D.V.A.); Contract grant sponsor: FWO-VI (Scientific Research, Flanders, Belgium; to K.H.); Contract grant sponsor: A-C Fabre was supported by a Fondation Fyssen postdoctoral fellowship.

*Correspondence to: Anthony Herrel; Département d'Ecologie et de Gestion de la Biodiversité, 55 rue Buffon, CP 55, 75005 Paris Cedex 5, France. E-mail: anthony.herrel@mnhn.fr

Received 3 January 2014; Revised 23 February 2014; Accepted 23 March 2014.

Published online 16 April 2014 in Wiley Online Library (wileyonlinelibrary.com). DOI 10.1002/jmor.20278

Lappin et al., 2006; Brecko et al., 2008; Vanhooydonck et al., 2010) the use of geometric morphometric approaches has been advocated for characterizing local shape differences that have functional consequences and are thus potentially under direct selection (Herrel et al., 2007; Kaliontzopoulou et al., 2007, 2008, 2012; Cornette et al., 2012, 2013). Geometric morphometric methods have many other advantages including the fact that they provide unbiased descriptions of shape in contrast to linear measurements (Zelditch, 2004). Especially at the level of the cranium and mandible, geometric morphometric techniques may be ideal to quantify the result of selection on different functional traits. For example, in the lizard *Anolis carolinensis*, it was suggested that the head shape differences between males and females detected using geometric morphometric approaches were related to differences in functional properties and diet (Herrel et al., 2007). Specifically, whereas males had larger adductor areas and relatively shorter rostra causing them to have higher bite forces, females had smaller adductor areas and relatively longer rostra which was suggested to be related to the inclusion of proportionally more evasive prey into the diet (Herrel et al., 2007).

Here, we explore whether the two approaches commonly used to characterize head shape differences between the sexes are similarly good descriptors of functional trait variation using the Argentine black and white tegu (*Tupinambis merianae*) as a model organism. Tegulizards are large omnivorous lizards that differ dramatically in body size, head size, and bite force between the sexes (Herrel et al., 2009; Naretto et al., 2013). However, whether the intersexual differences in bite force are simply the results of differences in head size or whether more subtle changes in the jaw muscle insertion areas exist that facilitate the observed differences in bite force remain currently unknown. Using the crania and mandibles of 19 lizards of known bite force, we use both linear and geometric morphometric approaches to test 1) whether intersexual differences in the shape of the cranium and mandible exist, 2) whether both approaches are equally powerful at detecting differences between the sexes, and 3) whether geometric morphometric approaches better insights into the underlying functional relationships with the jaw musculature generating bite force.

MATERIALS AND METHODS

Animals and Husbandry

Argentine black and white tegu, *T. merianae* (Duméril and Bibron, 1839) were obtained from the Jacarezário at the Universidade Estadual Paulista (Rio Claro, São Paulo, in southeastern Brazil), which runs a conservation breeding program for tegu lizards and other reptiles (Instituto Brasileiro do Meio Ambiente e dos Recursos Naturais Renováveis reg. 1-35-94-

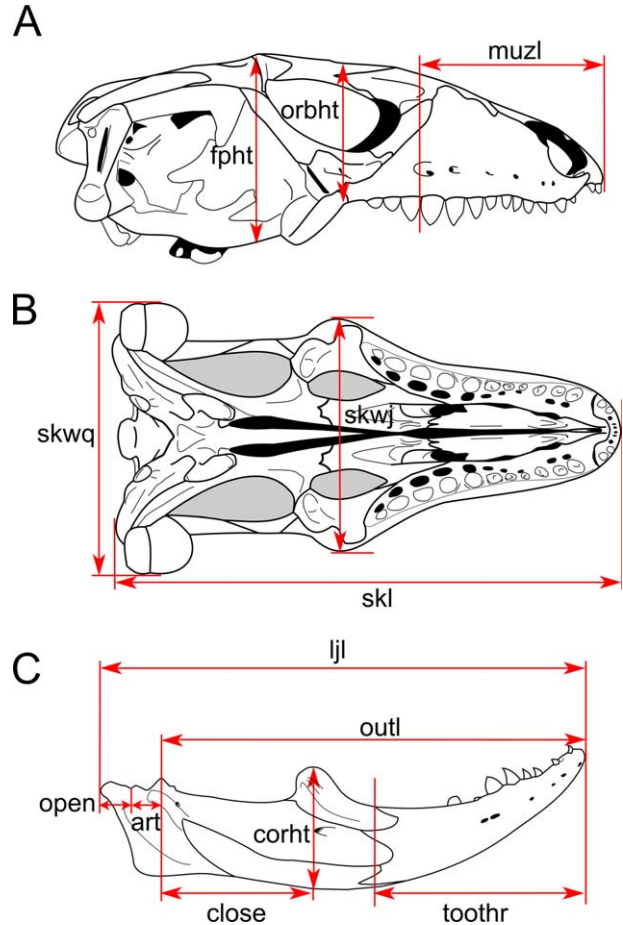


Fig. 1. *T. merianae*, schematic illustration of the cranium in dorsal (A) and ventral view (B), and the mandible in lateral view (C), illustrating the measurements taken to characterize variation in shape between the sexes. muzl, length of the cranium anterior to the orbit; orbht, height of the cranium at the level of the orbit; fpht, height of the cranium at the level of the fronto-parietal suture; skl, cranial length; skwj, cranial width at the level of the jugal; skwq, cranial width at the level of the quadrates; ljl, lower jaw length; outl, length of the mandible from the anteriormost aspect of the jaw joint to the tip of the jaw; toothr, toothrow length; corht, height of the mandible at the level of the coronoid; close, distance from the coronoid to the anteriormost aspect of the jaw articulation; art, length of the jaw articulation; open, distance from the back of the retroarticular process to the posteriormost aspect of the jaw articulation. [Color figure can be viewed in the online issue, which is available at wileyonlinelibrary.com.]

1088-8). Nineteen animals (10 males and nine females) of different ages were sacrificed for anatomical studies using an intramuscular injection of an overdose of pentobarbital after having their bite force recorded. Heads were dissected and skulls were cleaned by hand.

Linear and geometric morphometrics. The following linear dimensions (Fig. 1) were taken as detailed in Metzger and Herrel (2005) to the nearest 0.01 mm using digital calipers (Mitutoyo): cranium length (skl), muzzle length (muzl), cranium height at midorbit (orbht), cranium height at frontal-parietal suture (fpht), cranium width at the jugal (skwj), cranium width at the quadrate (skwq), lower jaw length (ljl), mandibular symphysis to anterior border of quadrate articular jaw joint (outl), toothrow length (toothr), length of jaw joint articulation (art), height at coronoid (corht), length of retroarticular process (open), and coronoid process to anterior border of jaw joint

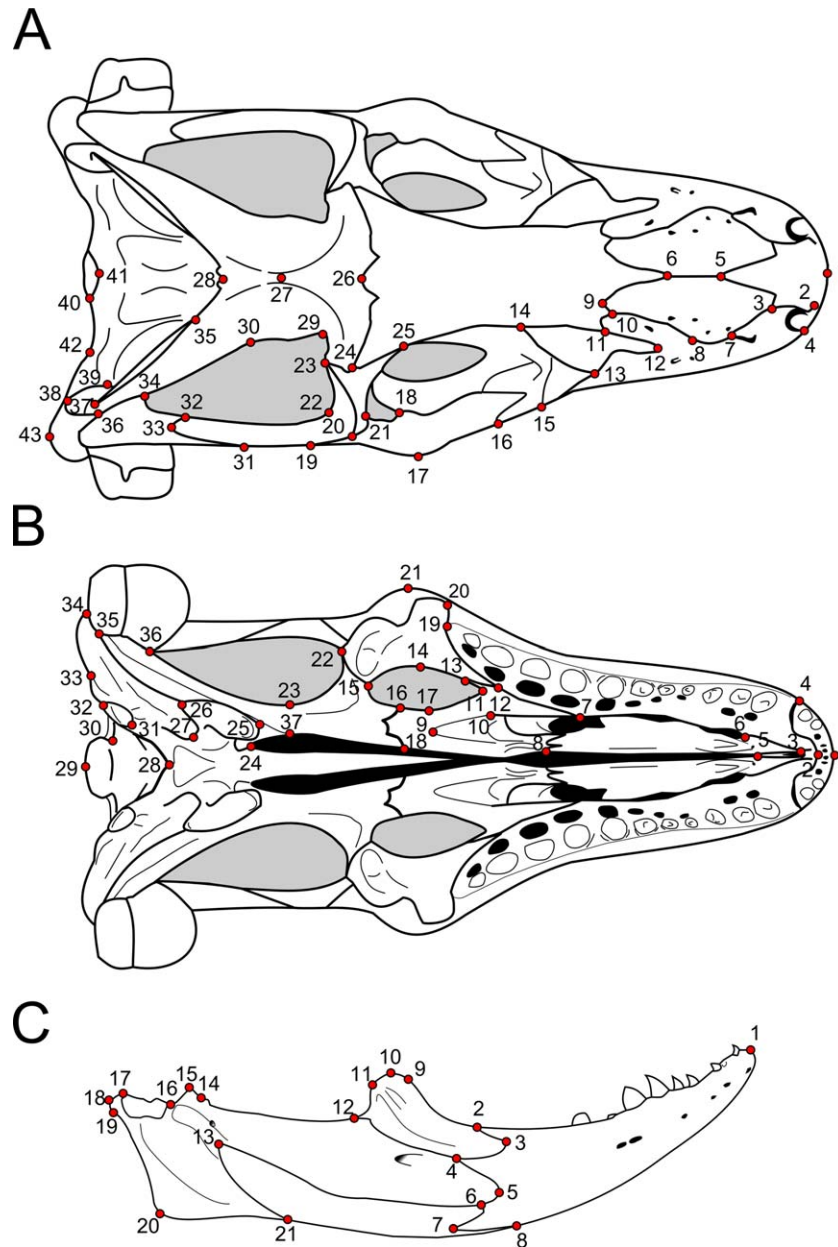


Fig. 2. *T. merianae*, schematic illustration of the cranium in dorsal (A) and ventral (B) view, and the mandible in lateral view (C) illustrating the landmarks taken for geometric morphometric analyses. Twenty-one landmarks were taken on the mandible, 42 on the dorsal view pictures of the cranium, and 40 landmarks on the ventral aspect of the cranium. [Color figure can be viewed in the online issue, which is available at wileyonlinelibrary.com.]

(close). These measurements were taken to reflect biomechanically relevant measures that should be related to bite force variation with the closing inlever (close) in theory being associated with higher bite forces. Similarly, a shorter outlever should also be reflected in an increase in bite force. One male individual was removed from the analysis of the linear dimensions as it was a clear outlier in jaw length relative to all others.

After measuring the specimens, pictures were taken in lateral view of the mandible and in dorsal and ventral views of the cranium with a grid as background for scaling purposes. On the dorsal cranial view, 27 Type I and 16 Type II landmarks were taken on one half of the cranium (Fig. 2, Table 1). On the ventral view, 23 Type I and 17 Type II landmarks were taken (Fig. 2, Table 2). On the mandible, 11 homologous Type I land-

marks and 10 Type II landmarks were taken (Zelditch, 2004; Fig. 2; Table 3). All landmarks were taken in TPSDig (V. 2.17, Rohlf, 2001a; available at: <http://life.bio.sunysb.edu/morph/>). Landmarks were always taken by the same person (A-CF). Two repetitions were done for each individual to assess measurement error, which was found to be low.

Bite forces. In vivo bite forces were measured using an isometric Kistler force transducer (9311B; range, ± 5000 N; Kistler, Switzerland) mounted on a purpose-built holder and connected to a Kistler charge amplifier (5995A; Kistler, Switzerland; see Herrel et al., 1999 for a more detailed description of the setup). Data used here are a subset of those presented in Herrel et al. (2009) and are summarized in Table 4.

TABLE 1. Definition of landmarks taken on the dorsal side of the cranium

Landmark	Definition
1	Antermost point of the premaxilla
2	Medial anterior intersection of the maxilla and premaxilla
3	Intersection between the premaxilla, the nasal and the maxilla
4	Lateral anterior intersection between the maxilla and the premaxilla
5	Most anterior point between the suture of the two nasal bones and the premaxilla
6	Most posterior point between the suture of the two nasal bones and the frontal
7	Point of maximum of curvature along the proximal part of the suture between the nasal and the maxilla
8	Point of maximal curvature along the distal part of the suture between the nasal and the maxilla
9	Point of maximum of curvature along the suture between the nasal and the frontal
10	Point of suture between the nasal, the maxilla and the frontal
11	Point of suture between the maxilla, the frontal and the prefrontal
12	Point of maximum of curvature anterior on the suture between the prefrontal and the maxilla
13	Point of suture between the prefrontal and the maxilla
14	Point of suture between the prefrontal and the frontal
15	Point of suture between the maxilla and the lacrymal
16	Most lateral point of the suture between the lacrymal and the jugal
17	Most lateral point of maximum of curvature of the jugal
18	Lateral point of the suture between the palatine and the jugal
19	Most lateral point of suture between the jugal and the squamosal
20	Lateral point of suture between the jugal, the squamosal, and the postorbital
21	Point of visual intersection between the ectopterygoid with the frontal
22	Most proximal lateral point of maximum of curvature of the squamosal
23	Suture between the squamosal, the postorbital and the parietal
24	Suture between the frontal, the postorbital and the parietal
25	Point of suture between the postorbital and the frontal
26	Point on the suture line between the frontal and the parietal at the midline
27	Point on the midline in the middle of the constriction of the parietal
28	Most distal point of the parietal along the midline
29	Most antero-medial point of maximum curvature the on the parietal
30	Most disto-medial point of maximum of curvature on the parietal
31	Most lateral point of suture between the squamosal and the supratemporal
32	Most medial point of suture between the squamosal and the supratemporal
33	Point of maximum of curvature on the supratemporal
34	Most proximal point of the suture between the supratemporal and the parietal
35	Most proximal point of the suture between the parietal and the exoccipital
36	Most distal point of suture between the parietal and the supratemporal
37	Point of maximum of curvature of the parietal
38	Most distal point on the suture between the parietal and the occipital
39	Most anterior point on the suture between the parietal and the occipital
40	Most lateral point of the foramen magnum
41	Most dorsal point of the foramen magnum along the midline
42	Point of maximum of concavity of the distal part of the occipital
43	Most distal point of the occipital

Analyses. Log-shape ratios (Mosimann and James, 1979) were calculated based of the raw \log_{10} -transformed linear dimensions of the jaw and mandible separately. Principal component analyses were run on the log-shape ratios and used to visualize differences between the sexes. Next, a multivariate analysis of variance (MANOVA) was run on the principal component scores representing 95% of the total variation. To explore phenetic similarity among individuals and between sexes we constructed neighbor joining trees using the principal components representing 95% of the total shape variation using the “ape” library in R (Paradis et al., 2012). Finally, we explored allometries present in the data set by regressing the shape variables of the principal component scores representing 95% of the total variation on the \log_{10} of overall size (i.e., the mean of all measurements for each individual after \log_{10} -transformation).

Shape variation of the cranium and mandible was subsequently quantified using geometric morphometric approaches allowing an analysis of size and shape components independently (Zelditch, 2004). Generalised Procrustes superimposition (Rohlf and Slice, 1990) was performed on the point coordinates using the package Rmorph (Baylac, 2012) in the program R (R Development Core Team, 2012). The Procrustes optimization

uses the superimposition of coordinates instead of distances providing the advantage over linear methods in controlling dimensional redundancy (Zelditch, 2004). Principal component analyses were run on the procrustes residuals and used to visualize differences between males and females. Next, principal components representing 95% of the total shape variation were used as input variables for a MANOVA to test for differences between the sexes in cranium and mandible shape in the program R (R Development Core Team, 2012) using the package “stats.” Neighbor joining trees were constructed using the Euclidean distances from the Procrustes tangent coordinates using the “ape” library in R (Paradis et al., 2012). We included the principal components that together represented 95% of the total shape variation of an analysis that used only the 18 individuals that were used in the linear morphometric analysis to allow a direct comparison between the results of the two types of approaches. Finally, we regressed shape (principal components representing 95% of the total shape variation) on centroid size (the only size variable statistically independent of shape; see Zelditch, 2004).

To explore whether both types of analyses predicted variation in performance equally well, we conducted a multiple

TABLE 2. Definition of landmarks taken on the ventral side of the cranium

Landmark	Definition
1	Anterior most point of the premaxilla along the midline
2	Point of maximum of concavity of the distal part of the premaxilla along the midline
3	Anterior most point of the vomer
4	Lateral most aspect of the suture between the premaxilla and the maxilla
5	Point of contact the two vomeral bones
6	Posterior point of contact between the vomer and the maxilla
7	Anterior most point along the suture between the maxilla and the palatine
8	Medial most point of the suture between the vomer and the palatine
9	Point of maximum of maximal curvature posterior on the palatine groove
10	Visual intersection between the groove and the lateral part of the palatine
11	Most anterior point of curvature of the suborbital fenestra
12	Intersection between the palatine, the maxilla and the ectopterygoid
13	Intersection between the palatine and the ectopterygoid
14	Most lateral point at the maximum of convexity of the suborbital fenestra
15	Most proximal, medial point of the suture between the ectopterygoid and the pterygoid
16	Most lateral point on the suture between the palatine and the pterygoid
17	Most medial point at the maximum of concavity of the suborbital fenestra
18	Most medial point of the suture between the palatine and the pterygoid
19	Point of maximum of curvature at the end of the tooth row on the suture between the maxilla and the ectopterygoid
20	Anterior intersection between the maxilla, the ectopterygoid and the jugal
21	Most lateral point of maximum of curvature of the jugal
22	Most lateral point of the suture between the ectopterygoid and the pterygoid
23	Most medial point of maximum of concavity of the pterygoid
24	Anterior most visual intersection between the quadrate and the pterygoid
25	Most anterior, medial point on the basisphenoid
26	Most posterior, lateral point on the basisphenoid
27	Anterior most point of the pretygoid basisphenoid articulation
28	Most posterior point of maximum concavity of the basisphenoid along the midline
29	Point of maximum of curvature of the occipital condyle along the midline
30	Most antero lateral point of the occipital condyle
31	Most anterior medial point of the insertion of the ventral neck muscles at the basioccipital
32	Most posterior lateral point of the insertion of the ventral neck muscles at the basioccipital
33	Point at the maximum of concavity on the most posterior part of the exoccipital
34	Most lateral point of contact between the exoccipital and the quadrate
35	Most medial point of contact between the exoccipital and the quadrate
36	Point of contact between the pterygoid and the quadrate
37	Point of contact between the pterygoid and the basisphenoid

regression of the principal components explaining 95% of the total variation on Log_{10} -transformed bite force.

RESULTS

Linear Morphometrics

A principal component analysis performed on the log-shape ratios of the linear cranium dimensions resulted in four axes together explaining 95% of the overall variation in the data set. A plot of the first two axes (Fig. 3A) showed an almost complete overlap between the two sexes. The first principal component (PC)-axis opposes the cranial height at frontal-parietal suture with the cranial width at the jugal. The second PC-axis opposes the cranial height at frontal-parietal suture with the cranial height at midorbit. A MANOVA performed on the cranial data did not demonstrate any differences between males and females (Wilks' lambda = 0.73, $F_{4,12} = 1.17$, $P = 0.36$). The principal component analysis performed on the log-shape ratios of the linear mandible dimensions resulted in four axes

together explaining 95% of the overall variation in the data set. In contrast to the cranium data, the first principal component (Fig. 3B) perfectly separated the two sexes. The first principal component axis opposes the inlever for jaw closing with the length of retroarticular process and the jaw outlever. The second principal component axis contrasts the outlever to the length of retroarticular process.

A MANOVA performed on the cranial data revealed significant differences between males and females (Wilks' lambda = 0.18, $F_{4,12} = 14.39$, $P < 0.001$). The neighbor joining trees constructed based on the principal components for the cranium and mandible visualized these differences with males and females being clustered on the two extremes of the tree only for the mandibular data set. Whereas a regression of cranial shape on bite force was not significant ($R^2 = 0.11$, $P = 0.81$), mandibular shape predicted bite force variation well ($R^2 = 0.88$, $P < 0.001$). Although allometries were not significant for cranial shape ($R^2 = 0.22$; $P = 0.47$), they were significant for mandibular shape ($R^2 = 0.89$; $P < 0.001$).

TABLE 3. Definition of the landmarks taken on the mandible

Landmark	Definition
1	Anterior most point of the dentary
2	Dorsal most dorsal point of suture between the dentary and the coronoid
3	Anterior most point of maximum of curvature on the suture between the dentary and the coronoid
4	Intersection between the dentary, the coronoid and the surangular
5	Anterior most point of maximum of curvature on the suture between the dentary and the surangular
6	Intersection between the dentary, the surangular and the angular
7	Posterior most point of maximum of curvature on the suture between the dentary and the angular
8	Ventral most point of contact between the angular and the dentary
9	Most antero dorsal point of curvature of the processus coronoideus
10	Most dorsal point of curvature of the processus coronoideus
11	Most postero dorsal point of curvature of the processus coronoideus
12	Posterior most intersection between the coronoid and the surangular
13	Most posterior point of curvature on the suture between the surangular and the angular
14	Point of maximum of concavity on the dorsal border of the surangular
15	Point at the most anterior tip of the articular
16	Point at the maximum of concavity of the articular
17	Most dorsal point of the retroarticular process
18	Most postero dorsal point of the retroarticular process
19	Most posterior ventral point of the retroarticular process
20	Most postero ventral point of the outline of the lower jaw
21	Point of contact between the angular and the articular

Geometric Morphometrics

A principal component analysis performed on the shape data of the cranium in dorsal view resulted in 12 axes together explaining 95% of the total variation in the data set. The first axis separated males from females (Fig. 4A) with males

having relatively larger adductor areas and relatively shorter rostra. A principal component analysis performed on the shape data of the cranium in ventral view resulted in 11 axes, together explaining 95% of the overall variation in the data set. Again, the first axis separated males from females

TABLE 4. Table summarizing the linear skull dimensions, bite forces, and snout-vent length for all individuals

ind	Sex	svl	bf	skl	skwq	skwj	orbht	fpht	muzl	ljl	toothr	corht	art	open	close	outl
69	Female	297	184.4	70.2	32.0	38.2	18.5	22.0	22.5	70.8	35.5	15.1	3.2	5.8	18.7	61.8
22	Female	300	233.6	80.4	37.4	45.9	19.7	26.9	29.1	79.0	38.8	18.0	4.1	6.2	22.1	100.2
14	Female	310	312.9	79.1	38.7	47.7	20.1	20.9	26.6	78.0	38.5	18.5	4.3	5.7	20.8	68.0
10	Female	322	185.5	72.1	32.4	40.4	16.3	22.7	23.6	72.4	35.5	16.0	3.7	5.8	19.8	73.8
40	Female	333	260.4	82.2	38.7	47.5	23.2	29.1	33.0	80.7	39.4	19.4	4.8	5.8	21.6	70.2
7	Female	335	235.8	76.2	35.0	45.0	16.9	23.5	24.5	76.3	37.1	16.6	3.8	5.5	20.9	64.0
72	Female	335	301.8	78.2	34.9	41.5	19.8	24.1	26.4	74.2	37.0	15.7	3.9	5.9	20.6	64.4
4	Female	345	228.0	81.4	39.7	47.2	19.4	26.4	26.9	79.8	37.6	18.5	3.7	7.0	21.4	69.1
42	Female	348	245.9	81.1	35.9	44.2	20.2	27.3	29.5	80.3	38.9	17.9	4.1	6.4	22.2	69.8
19	Male	270	240.3													
15	Male	357	278.3	83.7	38.1	48.8	21.0	28.6	27.8	85.4	39.3	19.2	5.2	7.3	23.6	73.0
27	Male	370	423.6	95.9	45.1	57.9	25.4	31.8	32.9	97.1	42.8	23.0	5.8	7.4	29.0	83.9
55	Male	372	357.7	93.7	41.6	54.6	21.3	29.5	32.5	94.5	41.7	23.6	5.5	7.2	28.8	81.8
1	Male	385	429.2	93.2	43.6	57.7	23.2	31.2	32.3	97.2	43.7	24.1	5.7	6.0	29.8	84.7
17	Male	385	411.3	97.4	44.2	55.5	22.1	30.2	33.1	99.2	48.1	23.5	5.3	6.2	30.9	87.6
50	Male	393	502.9	103.9	47.6	56.3	26.7	35.5	33.5	101.9	44.5	26.2	5.2	7.2	32.3	89.5
34	Male	405	464.9	112.3	49.9	60.6	27.0	36.7	38.2	113.7	50.4	26.9	6.2	7.2	36.8	71.0
39	Male	405	534.2	100.4	49.0	62.6	27.8	35.2	34.1	102.4	44.1	25.9	5.6	6.4	35.1	90.4
8	Male	425	451.5	111.4	51.1	58.8	27.6	37.9	39.7	109.8	51.4	28.4	5.9	7.1	35.1	96.8

All measurements are in mm except bite force which is in *N*. Individual 19 was used in the geometric morphometric analysis but was removed from the linear morphometric analysis.

Art, length of the jaw articulation; bf, bite force; close, distance from the coronoid to the anteriormost aspect of the jaw articulation; corht, height of the mandible at the level of the coronoid; fpht, height of the skull at the level of the fronto-parietal suture; ind, individual; ljl, lower jaw length; muzl, length of the skull anterior to the orbit; open, distance from the back of the retroarticular to the posteriormost aspect of the jaw articulation; orbht, height of the skull at the level of the orbit; outl, length of the mandible from the anteriormost aspect of the jaw joint to the tip of the jaw; skl, skull length; skwj, skull width at the level of the jugal; skwq, skull width at the level of the quadrates; svl, snout-vent length; toothr, toothrow length.

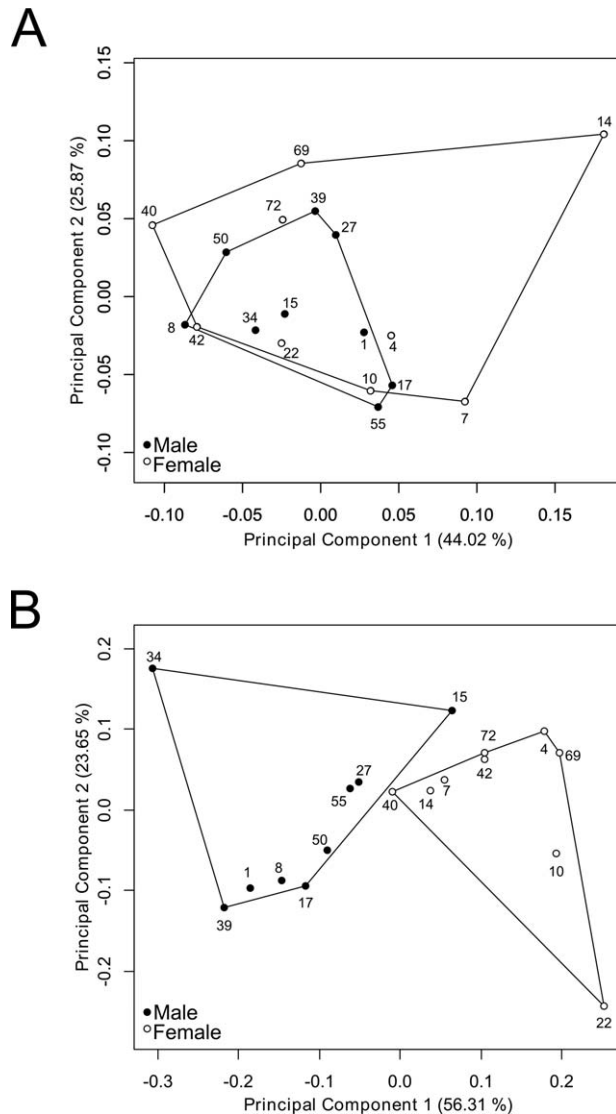


Fig. 3. Results of the linear morphometric analysis of the cranium (A) and mandible (B). Illustrated are the results of a principal component analysis performed on the Log-shape ratio data with males illustrated by filled circles and females by open circles. Whereas the mandible data separate the two sexes in shape space, the cranial data do not allow one to distinguish between the two sexes.

with males having relatively shorter rostra and larger adductor chambers than females. The principal component analysis performed on the shape data of the mandible in lateral view resulted in eight axes explaining 95% of the overall variation in the data set. The first axis again separated males from females with males having deeper mandibles and relatively shorter jaws. A MANOVA performed on the principal component scores for the axis explaining 95% of the shape variation detected significant differences between the sexes for the cranium in dorsal (Wilks' lambda = 0.013, $F_{12,2} = 29.77$, $P < 0.001$) and ventral view (Wilks' lambda = 0.015, $F_{11,3} = 35.35$, $P < 0.001$) as well as

for the mandible in lateral view (Wilks' lambda = 0.06, $F_{8,8} = 16.91$, $P < 0.001$). The neighbor joining trees constructed based on the principal components illustrated these differences with males and females being clustered on the two extremes of the tree. Regressions of cranial shape in dorsal ($R^2 = 0.85$; $P = 0.005$) and ventral view ($R^2 = 0.80$; $P = 0.005$) and of mandibular shape ($R^2 = 0.93$; $P < 0.001$) on bite force were highly significant. Allometries were significant for cranial shape in dorsal ($R^2 = 0.97$; $P < 0.001$) and ventral ($R^2 = 0.99$; $P < 0.001$) view as well as for mandibular shape ($R^2 = 0.98$; $P < 0.001$).

DISCUSSION

Whereas both linear and geometric morphometric approaches proved adequate for detecting differences between the sexes in the mandible (Fig. 3B), this was not the case for the cranium where geometric morphometric approaches clearly provide more insightful results. This suggests that the mandible is a better descriptor of intersexual shape differences than the cranium when using linear data, or alternatively, that the linear dimensions used for the mandible better reflect the parts of the bone directly related to functional differences between the sexes in bite force. Geometric morphometric approaches clearly allowed a discrimination between the sexes using either the cranium or the mandible independent of the variation in overall size of the individuals included in the data set. Specimens ranged from 30 to 35 cm snout-vent length (SVL) for females and from 27 to 43 cm SVL for males. Whereas the linear morphometric approaches based on jaw measures were unable to discriminate between the smallest male and the females included in our study, geometric morphometric approaches clearly identified this individual as male (Figs. 3, 5, and 6). Thus, geometric morphometric approaches allowed a discrimination of the sexes even at a relatively young age.

Unexpectedly, the linear cranial dimensions were rather poor descriptors of sex differences, despite the fact that they were chosen to reflect differences in biomechanically relevant properties such as the lengths of levers in the jaw system which should reflect underlying differences in the performance of the jaw system during biting. This observation may shed light on the results of Metzger and Herrel (2005), where only minor differences in cranial morphology were detected between lizards eating different types of food using the same linear cranial shape descriptors as in the present study. On the other hand, Stayton (2006) using geometric morphometric approaches detected clear convergence among herbivores in cranium shape suggesting that this approach may be better suited to characterize cranium shape in

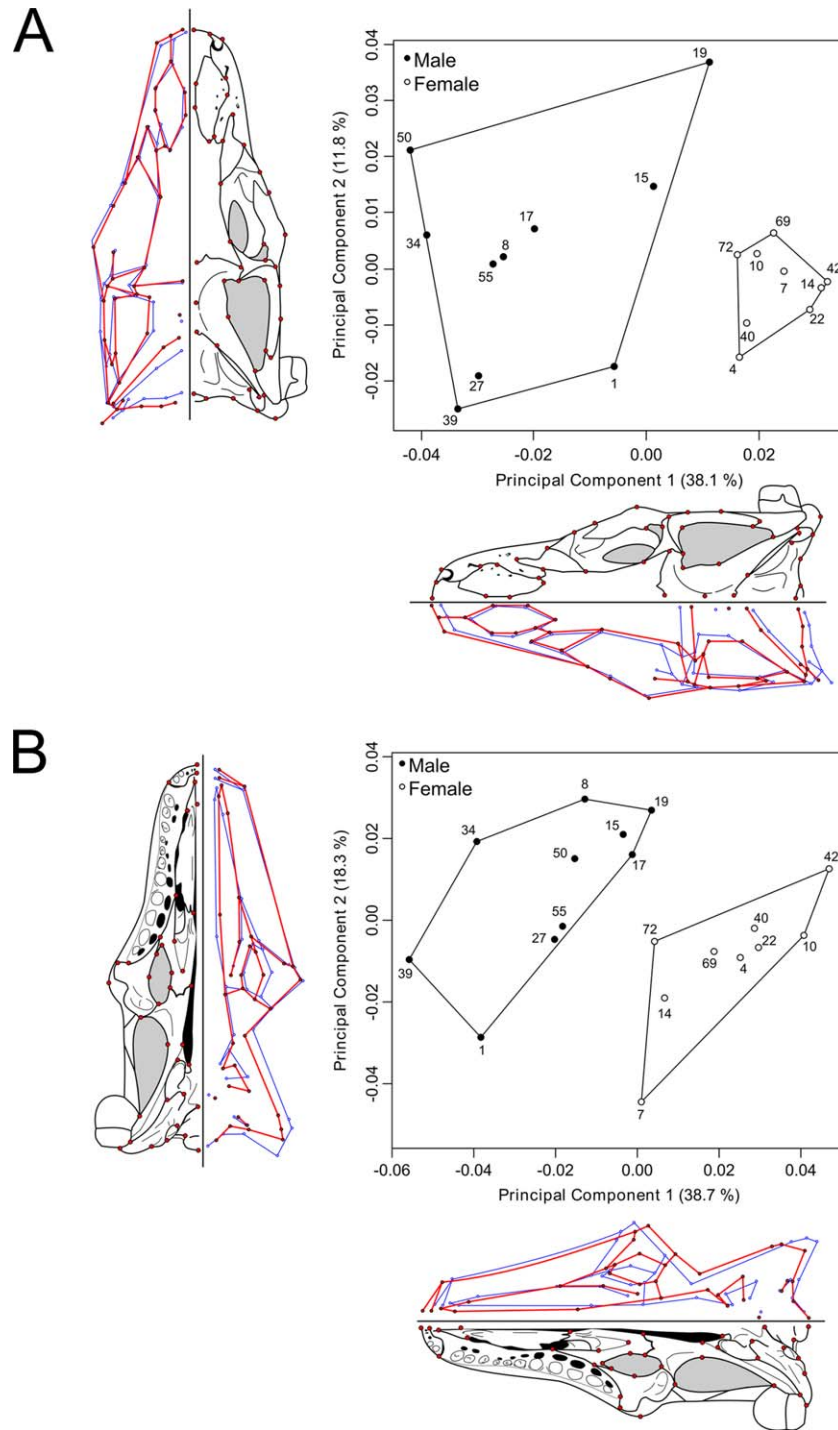


Fig. 4. Results of the geometric morphometric analysis of the cranium in (A) dorsal view, (B) ventral view. Illustrated are the results of a principal component analysis performed on the geometric morphometric data with males illustrated by filled circles and females by open circles. Below and to the left of the PC plot are illustrated a schematic view of the cranium and the deformation along the axes with the red shape representing the positive side of the axis and the blue shape representing the negative side of the axis. Males (in blue) have relatively larger adductor areas and a relatively shorter rostrum than females as can be observed in both dorsal and ventral view. Numbers represent the different individuals listed in Table 1. [Color figure can be viewed in the online issue, which is available at wileyonlinelibrary.com.]

lizards. Indeed, geometric morphometric approach provides a better shape description of the skull as it includes more variables (landmarks) than do lin-

ear methods. In contrast, however, many previous studies have demonstrated relationships between linear head dimensions and bite force and have

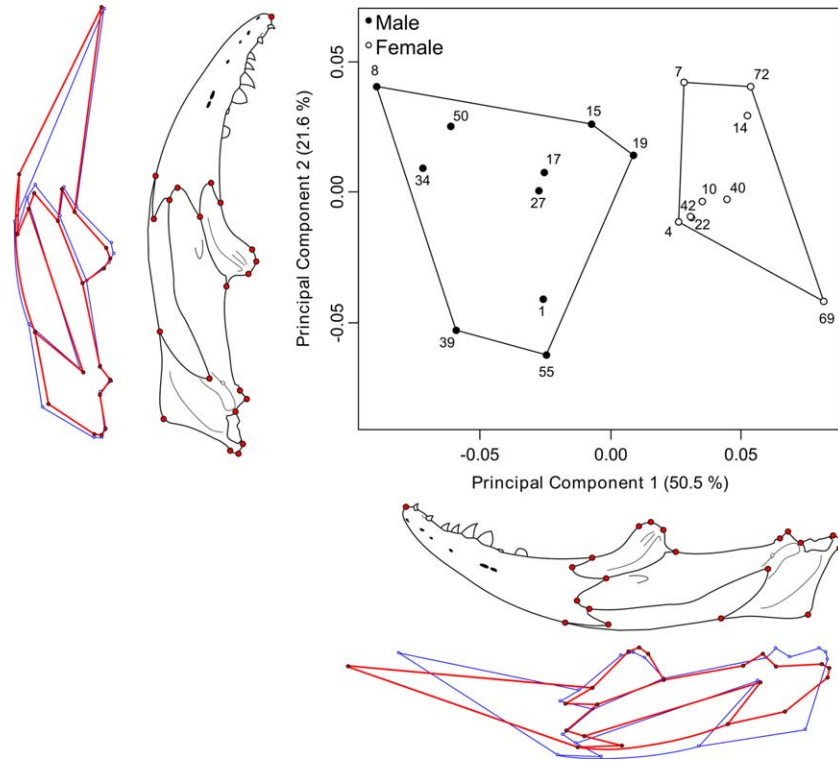


Fig. 5. Results of the geometric morphometric analysis of the mandible in lateral view. Illustrated are the results of a principal component analysis performed on the geometric morphometric data with males illustrated by filled circles and females by open circles. Below and to the left of the PC plot are illustrated a schematic view of the mandible and the deformation along the axes with the red shape representing the positive side of the axis and the blue shape representing the negative side of the axis. Males have relatively deeper, more curved, and shorter mandibles than females. Numbers represent the different individuals listed in Table 1. [Color figure can be viewed in the online issue, which is available at wileyonlinelibrary.com.]

shown differences in overall head dimensions between the sexes (e.g., Herrel et al., 1999; Lappin et al., 2006; Vanhooydonck et al., 2010). How to reconcile these differences? We suggest that the different results obtained may be due to the difference in measuring only the cranium (as in our study) versus the whole head. Indeed, whereas the cranium measures reflect simply the extent of the bones, measures of the whole head incorporate muscle bulging and may thus better reflect underlying functional differences. Alternatively, the difference may be due to the fact that most studies use absolute, nonsize-corrected head measures, whereas here we used “size-free” log-shape ratios to characterize variation in cranial dimensions. Note, however, that different data sets incorporate varying degrees of allometry which may affect the ability to detect shape differences between the two sexes.

Geometric morphometric approaches clearly highlighted differences between the sexes in areas that included muscle insertion areas suggesting that selection causing divergence between the sexes may act on functional traits such as bite force. Indeed, whereas the cranium of males was characterized by a slightly shorter snout and larger adductor area (Fig. 4), the mandible was characterized as being shorter and taller making

it more robust overall. These differences will have a direct affect on bite force with shorter snouts and mandibles reducing the outlever for biting and the larger adductor areas providing additional space for muscle insertion. The taller mandible likely both provides more space for muscle attachment as well as being more resistant to mechanical deformation induced during biting (Gröning et al., 2013). These observations suggest that at least the total jaw adductor mass should be different between the two sexes as has been suggested previously (Naretto et al., 2013). Moreover, our results show that cranial shape as characterized by geometric morphometrics is an excellent predictor of bite force with over 80% of the variation in the latter being predicted by cranial shape variation, whereas linear measures of the cranium were not significant predictors of bite force. With respect to the mandible, although both linear and geometric morphometric characterizations of shape were related to variation in bite force among individuals, geometric morphometric approaches were the better predictor of performance variation with 93% of the overall variation in bite force being explained by variation in mandibular shape.

In conclusion, our results suggest that geometric morphometric approaches are ideally suited to

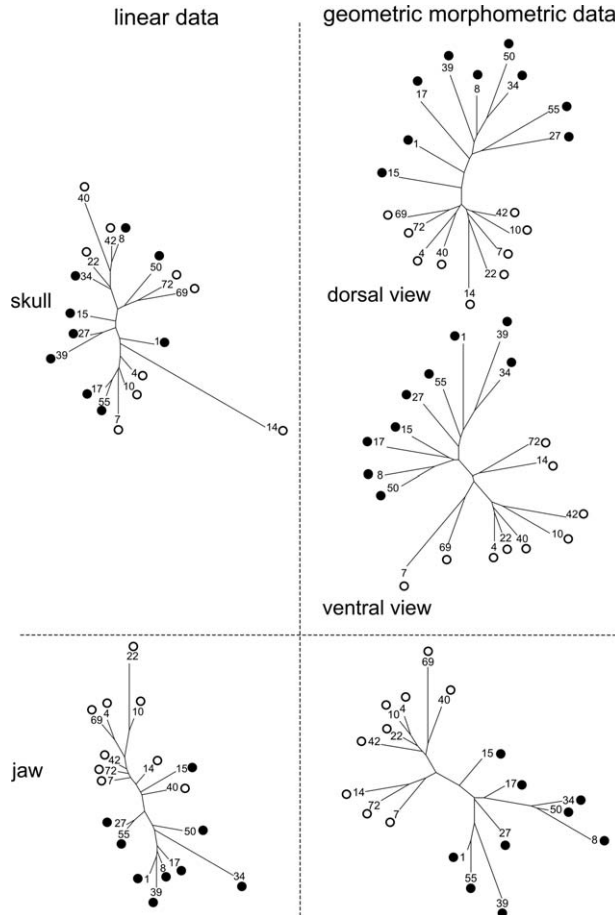


Fig. 6. Neighbor joining trees constructed using the principal components explaining 95% of the overall shape variation for the cranium (top) and the mandible (bottom) based on linear (left) and geometric (right) morphometric analyses. Filled circles represent males; open circles represent females. Whereas linear and geometric morphometric methods show similar results for the mandible, data for the cranium are noticeably different with linear morphometric approaches no longer distinguishing the two sexes. Numbers represent the different individuals listed in Table 1.

explore cranial and mandibular shape variation between sexes, at least among lizards. Moreover, this approach was able to detect variation in cranial and mandibular shape related to underlying functionally relevant traits such as bite force. Geometric morphometric approaches would also be ideally suited to further explore what muscles are most directly related to the observed shape differences between the sexes and thus likely under selection. This could further highlight whether selection is directly acting on muscles involved in biting such as the external adductors versus muscles that have been suggested to have a display function such as the external pterygoids (Herrel et al., 1999). Future studies combining geometric morphometric approaches coupled to biomechanical models are likely to provide significant insights into the proximate drivers of head shape variation between the sexes.

ACKNOWLEDGMENTS

The authors thank Jose Eduardo de Carvalho, Ananda Brito, and Carlos Carlos Navas for help in collecting the data, and two anonymous reviewers for constructive and helpful comments on an earlier version of the manuscript.

LITERATURE CITED

- Andersson M. 1994. *Sexual Selection: Monographs in Behavior and Ecology*. Princeton: Princeton University Press.
- Baylac M. 2012. Rmorph: A “R” Geometric Multivariate Morphometrics Library; baylac@mnhn.fr.
- Braña F. 1996. Sexual dimorphism in lacertid lizards: Male head increase vs female abdomen increase? *Oikos* 75: 511–523.
- Brecko J, Huyghe K, Vanhooydonck B, Herrel A, Grbac I, Van Damme R. 2008. Functional and ecological relevance of intraspecific variation in body size and shape in a lizard, *Podarcis melisellensis*. *Biol J Linn Soc* 94:251–264.
- Cornette R, Herrel A, Cosson J-F, Poitevin F, Baylac M. 2012. Rapid morpho-functional changes among insular populations of the greater white-toothed shrew. *Biol J Linn Soc* 107: 322–331.
- Cornette R, Baylac M, Souter T, Herrel A. 2013. Does shape covariation between the skull and the mandible have functional consequences? A 3D approach for a 3D problem. *J Anat* 223: 329–336.
- Gröning F, Jones MEH, Curtis N, Herrel A, O’Higgins P, Evans SE, Fagan MJ. 2013. The importance of accurate muscle modelling for biomechanical analyses: A case study with a lizard skull. *J R Soc Interface* 10:1742–5662. DOI: 10.1098/rsif.2013.0216.
- Herrel A, Spithoven L, Van Damme R, De Vree F. 1999. Sexual dimorphism of head size in *Gallotia galloti*; testing the niche divergence hypothesis by functional analyses. *Funct Ecol* 13: 289–297.
- Herrel A, McBrayer LD, Larson PM. 2007. Functional basis for intersexual differences in bite force in the lizard *Anolis carolinensis*. *Biol J Linn Soc* 91:111–119.
- Herrel A, Andrade DV, de Carvalho JE, Brito A, Abe A, Navas C. 2009. Aggressive behavior and performance in the tegu lizard *Tupinambis merianae*. *Physiol Biochem Zool* 82: 680–685.
- Herrel A, Castilla AM, Al-Sulaiti MK, Wessels JJ. 2014. Does large body size relax constraints on bite-force generation in lizards of the genus *Uromastyx*? *J. Zool* 292:170–174.
- Huyghe K, Vanhooydonck B, Scheers H, Molina-Borja M, Van Damme R. 2005. Morphology, performance and fighting capacity in male lizards, *Gallotia galloti*. *Funct Ecol* 19: 800–807.
- Kaliontzopoulou A, Carretero MA, Llorente GA. 2007. Multivariate and geometric morphometrics in the analysis of sexual dimorphism variation in *Podarcis* lizards. *J Morphol* 268: 152–165.
- Kaliontzopoulou A, Carretero MA, Llorente GA. 2008. Head shape allometry and proximate causes of head sexual dimorphism in *Podarcis* lizards: Joining linear and geometric morphometrics. *Biol J Linn Soc* 93:111–124.
- Kaliontzopoulou A, Adams DC, van der Meijden A, Perera A, Carretero MA. 2012. Relationships between head morphology, bite performance and ecology in two species of *Podarcis* wall lizards. *Evol Ecol* 26:825–845.
- Lappin AK, Husak JF. 2005. Weapon performance, not size, determines mating success and potential reproductive output in the collared lizard (*Crotaphytus collaris*). *Am Nat* 166:426–436.
- Lappin AK, Hamilton PS, Sullivan BK. 2006. Bite-performance and head shape in a sexually dimorphic crevice-dwelling

- lizard, the common chuckwalla [*Sauromalus ater* (= *obesus*)]. *Biol J Linn Soc* 88:215–222.
- Metzger KA, Herrel A. 2005. Correlations between lizard cranial shape and diet: A quantitative, phylogenetically informed analysis. *Biol J Linn Soc* 86:433–466.
- Mosimann JE, James FC. 1979. New statistical methods for allometry with application to Florida redwinged blackbirds. *Evolution* 33:444–459.
- Naretto S, Cardozo G, Blengini GS, Chiaraviglio M. Sexual selection and dynamics of jaw muscle in *Tupinambis* Lizards. *Evol Biol* 2013. DOI: 10.1007/s11692-013-9257-0.
- Paradis E, Bolker B, Claude J, Cuong HS, Desper R, Durand B, Dutheil J, Gascuel O, Heibl C, Lawson D, Lefort V, Legendre P, Lemon J, Noel Y, Nylander J, Oppen-Rhein R, Popescu A-A, Schliep K, Strimmer K, de Vienne D. 2012. Ape: Analyses of phylogenetics and evolution in R language. *Bioinformatics* 20: 289–290. R package version 3.0–5. Available at: <http://cran.r-project.org>, <http://ape.mpl.ird.fr/>. Accessed January 2014.
- R Development Core Team. 2012. R: A Language and Environment for Statistical Computing. Vienna: R Foundation for Statistical Computing.
- Rohlf FJ, Slice DE. 1990. Extensions of the Procrustes method for the optimal superimposition of landmarks. *Syst Biol* 39: 40–59.
- Stayton CT. 2006. Testing hypotheses of convergence with multivariate data: Morphological and functional convergence among herbivores. *Evolution* 60:824–841.
- Vanhooydonck B, Cruz FB, Abdala CS, Moreno Azócar DL, Bonino MF, Herrel A. 2010. Sex-specific evolution of bite performance in *Liolaemus* lizards (Iguania: Iguanidae): The battle of the sexes. *Biol J Linn Soc* 101:461–475.
- Vincent SE, Herrel A. 2007. Functional and ecological correlates of ecologically-based dimorphisms in squamate reptiles. *Integr Comp Biol* 47:172–188.
- Zelditch M. 2004. *Geometric Morphometrics for Biologists: A Primer*. Amsterdam: Elsevier, Academic Press.